

# Enhanced surface plasmon resonance detection using porous ITO–gold hybrid substrates

K.M. Byun · N.-H. Kim · J.W. Leem · J.S. Yu

Received: 22 September 2011 / Revised version: 16 January 2012 / Published online: 20 April 2012  
© Springer-Verlag 2012

**Abstract** We demonstrated enhanced surface plasmon resonance (SPR) detection by incorporating an indium tin oxide (ITO) layer on a thin gold film. Porous ITO layers were fabricated by e-beam evaporation and slanted deposition at room temperature and the ITO structure was optimized in terms of the surface roughness and the SPR curve characteristics. In sensing experiments, the results obtained by ethanol–water mixture test showed that SPR substrates with a porous ITO layer provided a notable sensitivity improvement compared to a conventional bare gold film, which is attributed to the nonlinear dispersion characteristic of surface plasmons. Our approach is intended to show the feasibility and extend the applicability of the porous ITO-mediated SPR biosensor to diverse biomolecular binding events.

## 1 Introduction

Optical detection technique based on surface plasmon resonance (SPR) has fascinated a large number of researchers because it is a very powerful tool for monitoring the binding interactions in biological systems [1]. When the wave vectors of the incidence beam and the surface plasmon are equal, the phenomenon of SPR takes place and the reflected

light intensity becomes completely attenuated. Since this SPR signal is sensitive to any variation in the refractive index or the thickness of a sensing medium around the metallic substrate, one can measure the adsorption of target analytes by tracking the change in the resonance condition. Typically, the metal film to excite the surface plasmons includes gold and silver. Gold has been the most widely used metal as it has stable optical and chemical properties. Although silver provides a sharp SPR curve, its disadvantage of a chemical instability makes the silver film difficult to get reliable optical signals and to perform long-time measurements [2].

Among various approaches which have been developed for improving the sensitivity of the SPR biosensor [3], the simplest way is to realize an extended surface-limited reaction area. In other words, by increasing the number of ligands and target molecules that participate in the binding interaction, we can produce a higher resonance shift. For example, Oh et al. reported a three-fold sensitivity improvement by utilizing a mesoporous silica structure with a high pore volume [4]. Thus, introduction of a rough and porous overlayer on the sensor surface can be an effective way for increasing the sensitivity because any corrugation, even at the nanometer scale, can provide more binding spaces than an ideally flat surface.

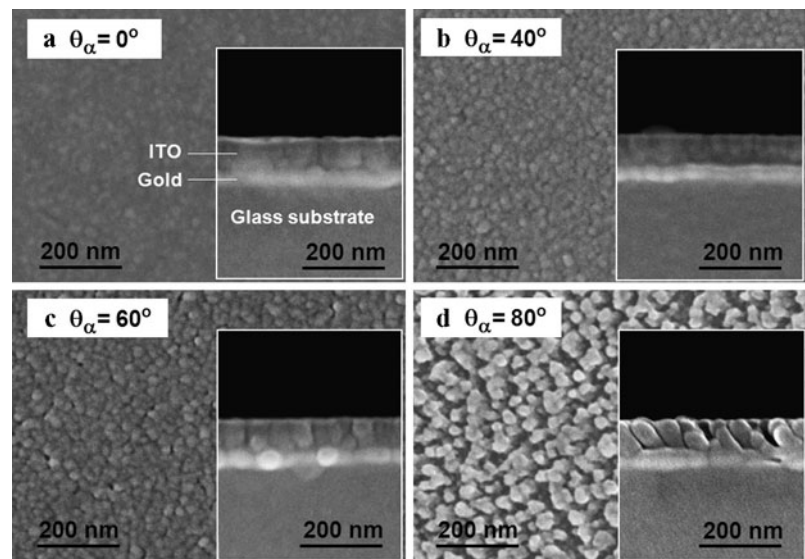
In this study, we intend to characterize the indium tin oxide (ITO)–gold hybrid substrate and explore its SPR sensing characteristics. The non-absorbing ITO films are free from the inevitable drawbacks that the use of metallic nanostructures or absorbing oxide coatings may cause. Due to a high imaginary part in refractive index of those absorptive materials, the SPR signals can be degraded by a broad curve width and a shallow minimum reflectance at resonance [2, 5]. The broad and shallow SPR curves increase the uncertainty of the sensor output and affect its high standard error in experimental measurement, finally resulting in a notable deterior-

---

K.M. Byun · N.-H. Kim  
Department of Biomedical Engineering, Kyung Hee University,  
1 Seocheon-dong, Giheung-gu, Yongin-si, Gyeonggi-do 446-701,  
Republic of Korea

J.W. Leem · J.S. Yu (✉)  
Department of Electronics and Radio Engineering, Institute for  
Laser Engineering, Kyung Hee University, 1 Seocheon-dong,  
Giheung-gu, Yongin-si, Gyeonggi-do 446-701, Republic of Korea  
e-mail: [jsyu@khu.ac.kr](mailto:jsyu@khu.ac.kr)  
Fax: +82-31-2062820

**Fig. 1** Cross-section and top-view SEM images of the deposited ITO layers on a thin gold film at incident flux angles of (a)  $\theta_\alpha = 0^\circ$ , (b)  $\theta_\alpha = 40^\circ$ , (c)  $\theta_\alpha = 60^\circ$ , and (d)  $\theta_\alpha = 80^\circ$ . The thicknesses of ITO and gold layers are fixed at 70 and 40 nm, respectively



ration of the detection limit. Hence, with an aim to improve the sensor performance of a traditional SPR detection, we propose the hybrid SPR structure by incorporating porous ITO layers on a planar gold film.

## 2 Experimental details

In order to find out if the ITO coating is a viable option for enhanced SPR detection, the first step is to determine whether we can make a thin ITO film with a high roughness. Using several fabrication techniques such as e-beam evaporation and angled deposition, we have attempted a formation of the ITO films on a gold/SF10 glass substrate. The target material is an ITO pellet with a composition of 90 wt.%  $\text{In}_2\text{O}_3$  and 10 wt.%  $\text{SnO}_2$  and the process pressure in the chamber is  $2 \times 10^{-5}$  torr at room temperature. To obtain rough and porous ITO films, the incident flux angle ( $\theta_\alpha$ ) is varied at  $\theta_\alpha = 0^\circ$ ,  $40^\circ$ ,  $60^\circ$ , and  $80^\circ$  without rotating the substrate. After the deposition which produces a porous columnar microstructure or nanostructure, the ITO films are annealed at  $500^\circ\text{C}$  by rapid thermal annealing in an air atmosphere. The fabricated samples are then cleaned in acetone and 70 % ethanol solution for 10 min in a sonication bath. Finally, the chip is rinsed with distilled deionized-water and irradiated by UV light to remove organic residues.

The characterization of the ITO-based SPR sample is performed with an in-house optical setup using an intensity-based angular interrogation scheme. Our setup employs a polarized He–Ne laser of  $\lambda = 633$  nm and dual rotation stages (URS75PP, Newport, Irvine, CA), prealigned for the sensor chip and a calibrated photodiode (818-UV, Newport, Irvine, CA), with a nominal resolution of  $0.002^\circ$ . During the experiments, SPR curves are measured with a resolution of  $0.01^\circ$ . The minimum detectable refractive index change of

the setup was estimated to be  $\Delta n \sim 1 \times 10^{-6}$  without any enhancement [6].

## 3 Results and discussion

Figure 1 shows the cross-section and top-view scanning electron microscope (SEM, LEO SUPRA 55, Carl Zeiss) images of the ITO films deposited on a 40-nm thick gold substrate with an incident flux angle of (a)  $\theta_\alpha = 0^\circ$ , (b)  $\theta_\alpha = 40^\circ$ , (c)  $\theta_\alpha = 60^\circ$ , and (d)  $\theta_\alpha = 80^\circ$ , respectively. The deposition rate of the ITO film varies depending on the  $\theta_\alpha$  in the range from 6.67 nm/min at  $\theta_\alpha = 0^\circ$  to 5.17 nm/min at  $\theta_\alpha = 80^\circ$ . Despite this contrast in deposition rate, it is found experimentally that a 70-nm thick ITO film could be obtained reproducibly for individual incident flux angles. At a fixed ITO thickness of 70 nm, the results in Fig. 1 present that the surface morphology of the ITO film is dependent on the tilted flux angle of  $\theta_\alpha$ . The average roughness ( $R_a$ ) measured from atomic force microscope (AFM, Dimension 3100, Veeco) is estimated to be  $R_a = 2.08$  nm for  $\theta_\alpha = 0^\circ$ ,  $R_a = 2.18$  nm for  $\theta_\alpha = 40^\circ$ ,  $R_a = 1.92$  nm for  $\theta_\alpha = 60^\circ$ , and  $R_a = 5.35$  nm for  $\theta_\alpha = 80^\circ$ . Hence, the highest surface roughness is obtained at the incident flux angle of  $\theta_\alpha = 80^\circ$  and its grain size is estimated to be 24.2 nm.

As a qualitative metric to determine an optimal deposition angle of the ITO film, we estimate the signal quality of the reflectance characteristics. Figure 2 presents the experimental reflectance spectra for the SPR samples with a 70-nm thick ITO layer. Among the four samples, the SPR curve for  $\theta_\alpha = 80^\circ$  shows the sharpest and the deepest resonance band, while the samples at  $\theta_\alpha = 0^\circ$  and  $40^\circ$  do not produce any significant SPR signals. Practically, as a broad curve width and a shallow SPR dip make it difficult to accurately detect the resonance position and to precisely an-

analyze the kinetics of binding events on a sensor surface, SPR sensing substrates with a sharp and deep resonance curve are highly desired. For efficient excitation of resonant surface plasmons, the Kretschmann configuration requires glass substrates with a refractive index larger than that of the dielectric medium surrounding a thin metal film [7, 8]. In our cases, the effective optical constants  $\varepsilon = (n, k)$  of the ITO layers are obtained to be (1.927, 0.032) for  $\theta_\alpha = 0^\circ$ , (1.851, 0.019) for  $\theta_\alpha = 40^\circ$ , (1.713, 0.007) for  $\theta_\alpha = 60^\circ$ , and (1.310, 0.002) for  $\theta_\alpha = 80^\circ$  at  $\lambda = 633$  nm using a spectroscopic ellipsometry (V-VASE, J.A. Woollam Co. Inc.). This measurement is consistent with our data in Fig. 2 because the ITO

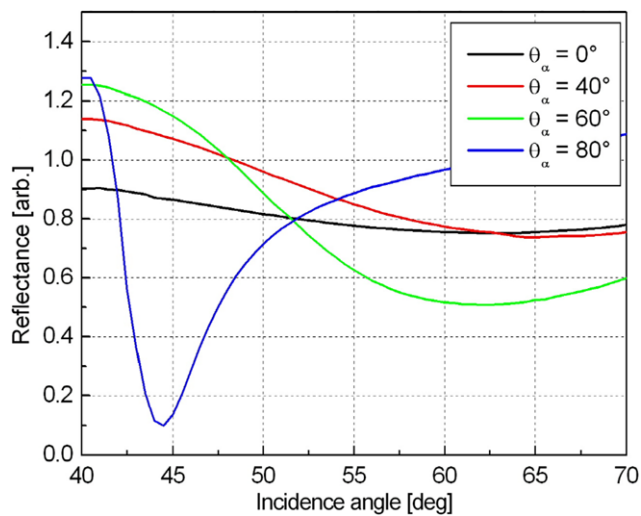


**Fig. 2** Experimental reflectance curves of the ITO-based SPR substrates at various incidence flux angles. The geometric parameters of individual samples are presented in Fig. 1

samples with no noticeable resonance signal have an effective refractive index larger than the value for the glass substrate ( $n_{\text{SF10}} = 1.723$  at  $\lambda = 633$  nm [9]). As a result, when taking both the surface roughness and the SPR curve characteristics into consideration, the optimal ITO layer is determined as the one with the incidence flux angle of  $\theta_\alpha = 80^\circ$ .

After optimizing the experimental conditions of the porous ITO structures at  $\theta_\alpha = 80^\circ$ , we fabricate three working samples: one planar gold film and two ITO–gold hybrid substrates. By changing the deposition time, 45-nm and 90-nm thick ITO layers are obtained and denoted by Samples A and B, respectively. The mean roughness is determined as  $R_a = 3.93$  nm for Sample A and 6.71 nm for Sample B. As a control, a bare gold film sputtered onto a  $20 \times 20$  mm<sup>2</sup> SF10 glass substrate has a roughness of  $R_a = 1.08$  nm. From the  $5 \times 5$   $\mu\text{m}^2$  AFM scan images in Fig. 3, the slanted ITO deposition yields a substantially rough and porous dielectric film on the sensor surface over a large area.

Figure 4 shows the SPR characteristics obtained from Samples A and B theoretically and experimentally when the porous ITO layer has a contact with air and water media. We utilize a transfer-matrix method (TMM) to calculate the reflectance characteristics of the fabricated SPR samples. The TMM has been extensively used and well-validated for calculation of the multilayered optical systems. For details on our TMM routine, readers are advised to refer to Ref. [10]. In this TMM calculation, the optical constants  $\varepsilon = (n, k)$  of SF10 and gold are set to be (1.723, 0) and (0.18, 3.00) at  $\lambda = 633$  nm [8]. The refractive indices of the air and water media are assumed to be 1.00 and 1.33. According to the Bruggemann effective medium approximation [11], the

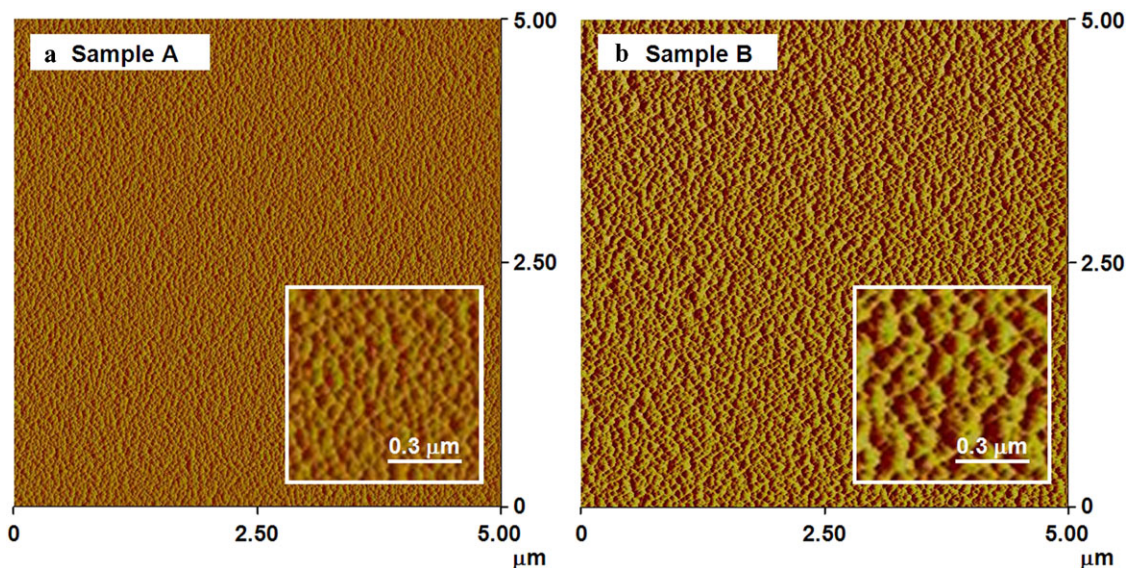


**Fig. 3** AFM images of the fabricated samples with (a) 45-nm and (b) 90-nm thick ITO film at  $\theta_\alpha = 80^\circ$ . The measured average roughness is estimated to be 3.93 nm for Sample A and 6.71 nm for Sample B while a bare gold film has a mean roughness of 1.08 nm

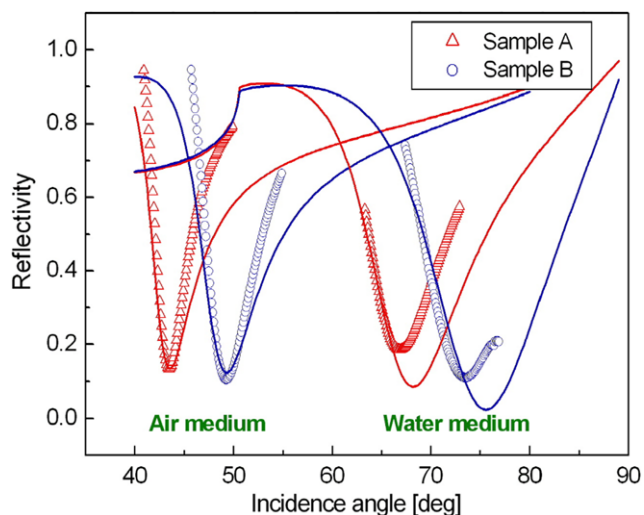


**Fig. 4** Experimental reflectivity versus incidence angle curves for Sample A (red triangle) and Sample B (blue circle) in both air and water media. The solid lines indicate the calculated SPR curves

following expression holds for the effective refractive index  $n_{\text{eff}}$  of the porous ITO layer:

$$f_{\text{ITO}} \frac{n_{\text{ITO}}^2 - n_{\text{eff}}^2}{n_{\text{ITO}}^2 + 2n_{\text{eff}}^2} + (1 - f_{\text{ITO}}) \frac{n_{\text{env}}^2 - n_{\text{eff}}^2}{n_{\text{env}}^2 + 2n_{\text{eff}}^2} = 0, \quad (1)$$

where  $n_{\text{env}}$  is the refractive index of the medium filling the pores within the porous ITO films.  $f_{\text{ITO}}$  and  $n_{\text{ITO}}$  are the volume fraction of the deposited ITO film and the refractive index of the homogeneous ITO layer with a zero porosity, respectively. From our previous literature [12], the vertically deposited ITO film at  $\theta_\alpha = 0^\circ$  showed a zero porosity and its refractive index was  $n_{\text{ITO}} = 1.93$  at  $\lambda = 633$  nm. Also, the volume fraction of ITO was approximately  $f_{\text{ITO}} \sim 0.35$  at  $\theta_\alpha = 80^\circ$ . Using Eq. (1),  $n_{\text{eff}}$  is calculated to be 1.31 in air environments (i.e.,  $n_{\text{env}} = 1.00$ ) and this value matches well with the previously measured refractive index of the porous ITO film [12]. In water ambience of  $n_{\text{env}} = 1.33$ , the effective refractive index is determined as  $n_{\text{eff}} = 1.53$ . In Fig. 5, linear regression analysis demonstrates that  $n_{\text{eff}}$  in response to an increasing  $n_{\text{env}}$  is extremely linear for a wide range of  $n_{\text{env}}$  with  $R = 0.99996$ . Here,  $R$  is the correlation coefficient that denotes the linearity obtainable in the performance measure.

The SPR curves in Fig. 4 show that the experimental results are in good agreement with the numerical data in both Samples A and B, especially for air environments. In water ambience, there is a slight discrepancy between the measured and calculated SPR characteristics. This is probably attributed to the inaccessibility of water molecules into the vacant pores relatively far away from the ITO–water interface. In other words, as inherent structural defects can prevent water molecules from permeating deeply through the porous ITO film, some pores may remain as air-filled cavities and thus, an actual effective refractive index  $n_{\text{eff}}$  in water

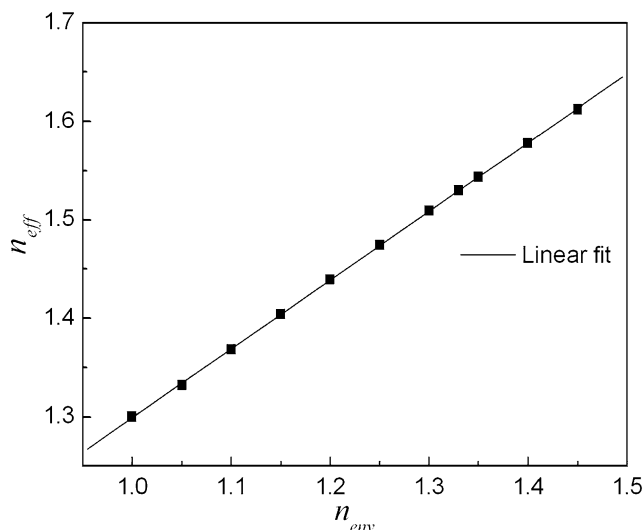


**Fig. 5** Linear regression analysis between the effective refractive index of porous ITO layers ( $n_{\text{eff}}$ ) and the refractive index of dielectric medium ( $n_{\text{env}}$ )

medium can be slightly smaller than the value determined theoretically by Eq. (1).

An advantageous aspect of the non-absorptive ITO film is also exhibited in Fig. 4. It has been found from the previous studies that the use of absorptive materials such as metallic nanostructures or absorbing dielectric coatings for achieving a corrugated sensor surface makes the SPR curve broader and shallower significantly due to their nonzero imaginary dielectric components [2, 5]. These changes in the SPR characteristics resemble the dramatic variations in the SPR signal induced by colloidal gold nanoparticles [13]. The broad and shallow SPR curves increase the uncertainty of the sensor output and affect its high standard error in experimental measurement, finally producing a notable degradation of the detection limit. On the other hand, the porous ITO film with a good optical transparency can be an effective candidate for protecting the signal quality from being highly degenerated as well as for providing an increased binding area.

Subsequently, we estimate the sensor sensitivity of the ITO-mediated SPR substrates by measuring the dependence of the SPR angle shift on the refractive index change of surrounding aqueous medium. The refractive index change measured by a refractometer (2010/M, Metricon Corporation, USA) is  $\Delta n = 0.03$  at  $\lambda = 633$  nm with an increase of the concentration of ethanol mixture from 0 % for pure water. In Fig. 6, the resonance angles before and after the refractive index change are  $59.61^\circ$  and  $61.86^\circ$  for bare gold substrate; thus, the resonance shift is  $2.25^\circ$ . On the other hand, ITO-based samples exhibit an enhanced SPR shift with an increase of the ITO thickness. The sensitivity enhancement factor (SEF), defined as  $\Delta\theta_{\text{SPR}}(\text{with ITO films})/\Delta\theta_{\text{SPR}}(\text{without ITO films})$ , is de-

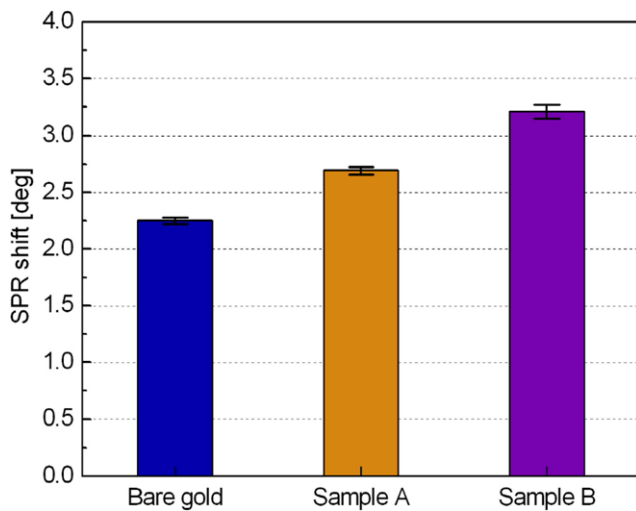
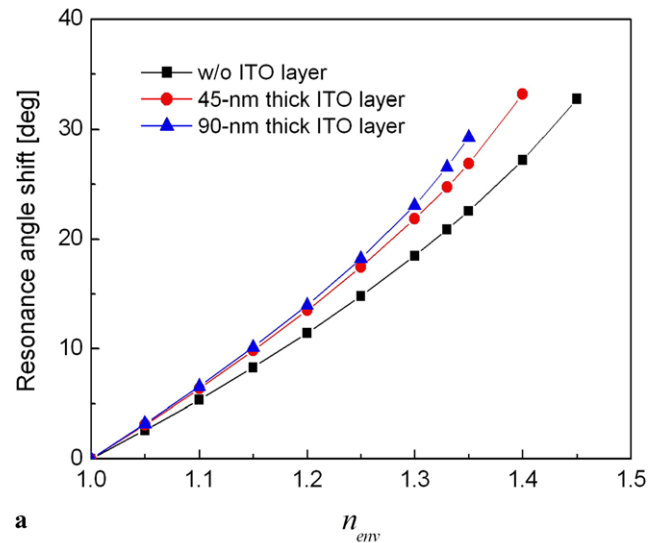


**Fig. 6** Statistical data of the SPR angle shift of the three working samples for ethanol–water mixture experiments. The resonance shift is determined to be  $2.25^\circ \pm 0.029^\circ$  for a bare gold film,  $2.69^\circ \pm 0.032^\circ$  for Sample A, and  $3.21^\circ \pm 0.058^\circ$  for Sample B, indicating a 20 % and 43 % improvement in sensitivity, compared to a traditional SPR scheme

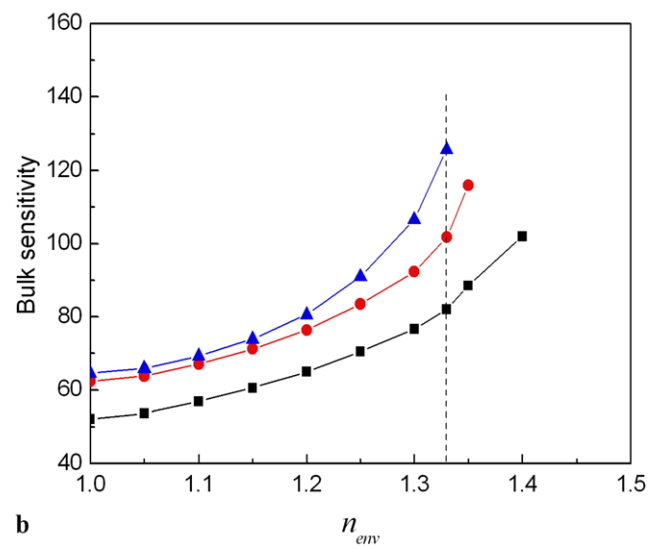
terminated to be 1.20 for Sample A and 1.43 for Sample B, indicating a 20 % and 43 % increase in sensitivity.

While the amount of the measured SEF is less significant, it should be emphasized that the results obtained from bulk ambient change are quite contrary to our expectations. Since the volume occupied by the porous ITO layers makes the overall refractive index change of bulk ambience volume smaller than the case of the conventional SPR structure without ITO layers, it has been expected that the proposed ITO-based SPR samples would sense less refractive index change when the bulk environment is exchanged. However, the ITO-based samples presented enhanced SPR responses to bulk ambience exchange and it seems that the nonlinear characteristic of a dispersion relation of surface plasmons is responsible for such results [14, 15].

To consider this theoretically, a refractive index of the bulk ambience is assumed to change at a sufficiently wide range from 1.00 to 1.45 with an interval of 0.05. The numerical data calculated by TMM and effective medium approximation in Fig. 7(a) show that for a bulk environment exchange, the SPR samples with and without ITO layers present a nonlinear increment of SPR angle. Also, as shown in Fig. 7(b), a slope of the resonance shift, indicating bulk sensitivity, becomes stiffer with an increasing refractive index and the maximum bulk sensitivity is obtained at the Sample B. At the refractive index of 1.33, the bulk sensitivities are found to be 82.1 for bare gold sample, 101.8 for Sample A, and 125.8 for Sample B, implying a 24 % and 53 % enhancement. These results are fairly consistent with the SEF values obtained experimentally in Fig. 6.



**a**



**b**

**Fig. 7** (a) Resonance angle shift and (b) bulk sensitivity characteristics for the three working samples when the refractive index of environment increases from 1.00 to 1.45 in steps of 0.05

Additional analytical calculation also supports the validity of our plasmonic interpretation. From a dispersion relation of surface plasmons, the bulk sensitivity  $S$  can be approximated as

$$S = \frac{\partial \theta_{SPR}}{\partial n_{env}} \approx \left(1 - \frac{\epsilon_d}{\epsilon'_m}\right) \frac{1}{\sqrt{n_S^2 - \epsilon_d}}, \tag{2}$$

where  $\epsilon'_m$ ,  $\epsilon_d$ , and  $n_S$  are the real part of the permittivity of a metal, the permittivity of dielectric medium, and the refractive index of a glass substrate, respectively. The equation suggests that the bulk sensitivity should present a super-linear dependence on  $n_{env}$ , i.e.,  $S$  increases faster than  $n_{env}$  does. In particular, when a dielectric ITO layer is formed between substrate and environment, the bulk sensitivity is increased with the thickness of ITO layer because the growing

thickness causes a permittivity of dielectric medium on the metal film to be effectively increased, finally resulting in a further increase of  $S$ . As a result, use of thin dielectric layers can be a simple but effective way for enhancing the sensor sensitivity in multilayered SPR configurations [16, 17].

In an actual application, most of biomolecular interactions generally lead to a very small change of refractive index in a highly limited volume in the vicinity of the sensor surface. Therefore, the small-signal sensitivity obtained from the layered biointeractions such as the formation of self-assembled monolayers and DNA hybridization could be a more practical performance measure of the fabricated ITO–gold substrates [15]. However, as the immobilization efficiency of the capture ligands is varied according to the substrate material, layered biointeractions may not produce an identical refractive index change between gold and porous ITO surfaces. While the experiments using layered binding reactions could not be performed, we believe that the SEFs obtained from the ethanol–water mixture test are close to the worst-case results and the practical sensor performance of the porous ITO layers can be improved more significantly by the surface-limited binding events [18, 19].

#### 4 Conclusion

In this study, we presented the fabrication and characterization of the porous ITO–gold hybrid SPR substrates. Using TMM and effective medium approximation, the fabricated SPR samples were analyzed theoretically and the computation results were consistent well with the experimental data. From ethanol–water mixture test, a promising potential of the porous ITO films for enhanced SPR detection was demonstrated. Due to the simplicity in fabrication, it is expected that ITO layers with a high porosity could be used to augment the surface binding area, therefore providing an improved sensitivity for a variety of biomolecular detection.

**Acknowledgements** Kyung Min Byun and Jae Su Yu acknowledge the support of Basic Science Research Program through the National Research Foundation of Korea (NRF) funded by the Korean government (MEST) (2011-0029485 and 2011-0003857, respectively).

#### References

1. J. Homola, S.S. Yee, G. Gauglitz, *Sens. Actuators B* **54**, 3 (1999)
2. S. Szunerits, X. Castel, *J. Phys. Chem. C* **112**, 15813 (2008)
3. K.M. Byun, *J. Opt. Soc. Korea* **14**, 65 (2010)
4. S. Oh, J. Moon, T. Kang, S. Hong, J. Yi, *Sens. Actuators B* **114**, 1096 (2006)
5. W.P. Hu, S.J. Chen, K.T. Huang, J.H. Hsu, W.Y. Chen, G.L. Chang, K.A. Lai, *Biosens. Bioelectron.* **19**, 1465 (2004)
6. K.M. Byun, S.J. Yoon, D. Kim, S.J. Kim, *Opt. Lett.* **32**, 1902 (2007)
7. V.M. Shalaev, S. Kawata, *Nanophotonics with Surface Plasmons* (Elsevier, Amsterdam, 2007), Chap. 8
8. S.J. Yoon, D. Kim, *J. Opt. Soc. Am. A* **25**, 725 (2008)
9. E.D. Palik, *Handbook of Optical Constants of Solids* (Elsevier, Amsterdam, 1985)
10. S.H. Choi, K.M. Byun, *J. Opt. Soc. Am. A* **27**, 2229 (2010)
11. H.Y. Chen, H.W. Lin, C.Y. Wu, W.C. Chen, J.S. Chen, S. Gwo, *Opt. Express* **16**, 8106 (2008)
12. J.W. Leem, J.S. Yu, *Opt. Express* **19**, 258 (2011)
13. L. He, M.D. Musick, S.R. Nicewarner, F.G. Salinas, S.J. Benkovic, M.J. Natan, C.D. Keating, *J. Am. Chem. Soc.* **122**, 9071 (2000)
14. H. Raether, *Surface Plasmon on Smooth and Rough Surfaces and on Gratings* (Springer, Berlin, 1988)
15. K.M. Byun, S.M. Jang, S.J. Kim, D. Kim, *J. Opt. Soc. Am. A* **26**, 1027 (2009)
16. A. Lahav, M. Auslender, I. Abdulhalim, *Opt. Lett.* **33**, 2539 (2008)
17. A. Shalabney, I. Abdulhalim, *Sens. Actuators A* **159**, 24 (2010)
18. K. Kim, D.J. Kim, S. Moon, D. Kim, K.M. Byun, *Nanotechnology* **20**, 315501 (2009)
19. T. Kan, K. Matsumoto, I. Shimoyama, in *International Solid-State Sensors, Actuators and Microsystems Conference, 2009*, TRANSDUCERS 2009 (2009), p. 1481